

Realtime Multi-User Multi-Antenna Downlink Measurements

T. Wirth, V. Jungnickel, A. Forck, S. Wahls, H. Gaebler
 Fraunhofer Institute f. Telecommunications
 Heinrich-Hertz-Institut,
 Einsteinufer 37, D-10587 Berlin, Germany

T. Haustein, J. Eichinger, D. Monge, E. Schulz
 Nokia Siemens Networks GmbH & Co.KG
 St. Martinstraße 76,
 D-81617 Munich, Germany

C. Juchems, F. Luhn, R. Zavrtak
 IAF GmbH
 Berliner Straße 52J,
 D-38104 Braunschweig, Germany

Abstract— In this paper, we present real-time broadband multi-user multi-antenna measurements in typical indoor and outdoor scenarios. For the first time, essential frequency-selective functions of a new medium access control (MAC) layer, namely fair resource assignment to multiple users, spatial mode selection and adaptive modulation, have been implemented in real-time on standard digital signal processing hardware. The new MAC layer is steered over wireless feedback and control channels in a closed loop manner. Our implementation uses parameters close to the forthcoming long-term evolution (LTE) of the 3G air interface, thus illustrating the feasibility of the new functions in next-generation cellular radio systems. The paper describes our real-time implementation and reports several test results. Benefits of the frequency-selective multi-user MIMO MAC are validated in realistic mobile propagation environments.

I. INTRODUCTION

There are several new technologies in the physical layer (PHY) and medium access control layer (MAC) of next generation mobile communication systems, as multiple-input multiple-output (MIMO) and orthogonal frequency division multiple access (OFDMA). The potential of these new technologies is evident from numerous simulation studies in the existing literature, and they are already part of emerging cellular standards.

However, these new techniques require the real-time implementation of some new and highly complex signal processing algorithms, i.e. MIMO-OFDMA at the PHY layer, and the realization of functional feedback and control channels in uplink and downlink directions, in order to transport resource requests and grant lists timely in a closed loop manner. Moreover, an implementation of intelligent scheduling algorithms is needed in combination with a highly flexible mapping of data symbols onto granted resources at the MAC layer. Some of these new components have been previously tested, see MIMO-OFDM [1] or multi-user scheduling on a single carrier in [2]. However, the complete set of algorithms has never before been integrated in real-time and tested over the air in a realistic cellular scenario.

In this paper, we demonstrate the feasibility of new multi-user MIMO MAC algorithms in real-time and illustrate the potential spectral efficiency gains of these new technologies under real-world conditions. The paper is organized as follows. In **Sect. II**, essential algorithms used at the PHY and MAC

layer are summarized. In **Sect. III**, our real-time implementation is summarized. In **Sect. IV**, we describe the 2 scenarios where multi-user measurements have been conducted. The measurement results are described in **Sect. V**.

II. FUNCTIONAL DESCRIPTION OF PHY AND MAC

A. Physical Layer

The physical layer (PHY) is based on MIMO-OFDMA in the downlink and single-carrier (SC-) FDMA in the uplink. With OFDMA, data signals are directly mapped in frequency domain onto multiple subcarriers. The transmission equation on each subcarrier is given by:

$$\mathbf{y}_n = \mathbf{H}_n \cdot \mathbf{x}_n + \mathbf{n}_n \quad (1)$$

where \mathbf{y}_n is the received signal vector on subcarrier n , \mathbf{H}_n the n -th MIMO channel matrix with coefficients for each link between all transmit and receive antennas, \mathbf{x}_n is the transmitted symbol vector on subcarrier n and \mathbf{n}_n the noise vector. Signals are transformed to time domain using the inverse fast fourier transform (IFFT). With SC-FDMA, the data are passed through an N-point discrete fourier transform (DFT) before they are mapped onto the subcarriers. A cyclic prefix is added after the IFFT and the signal is transmitted over the air interface. The transmitter supports two spatial modes: single-stream or multi-stream. For single-stream transmission, either the first or the second transmit antenna is used. For multi-stream transmission, the elementary transmission chains are copied for each antenna and both chains are used consecutively. At the receiver, either single-stream or multi-stream equalization is used prior to detecting the data. Single-stream equalization uses maximum ratio combining (MRC), as in

$$\tilde{\mathbf{x}}_n = \mathbf{H}_n^H \mathbf{y}_n. \quad (2)$$

Multi-stream equalization is done using the linear minimum mean square error (MMSE) detector, denoted by

$$\tilde{\mathbf{x}}_n = \mathbf{H}_n^H \cdot [\sigma^2 \mathbf{I} + \mathbf{H}_n \mathbf{H}_n^H]^{-1} \cdot \mathbf{y}_n \quad (3)$$

Here, $\tilde{\mathbf{x}}_n$ is the estimated symbol vector on subcarrier n , σ^2 the noise power, \mathbf{H}_n the channel matrix, $(\cdot)^H$ stands for the Hermitian transpose and \mathbf{I} for the identity matrix.

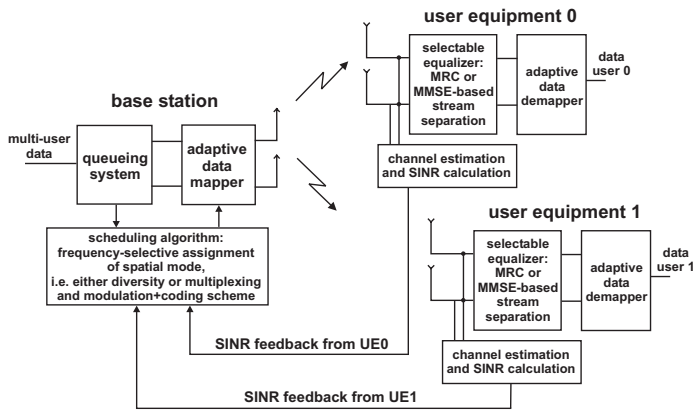


Fig. 1. Overview: System Implementation

As an interface to the MAC, the PHY calculates at the receive side for each spatial mode the signal-to-noise-and-interference ratio (SINR) in front of the QAM demodulator. The solution for the SINR for antenna i at a particular subcarrier with given transmission powers ($p_1 \cdots p_L$), channel vector \mathbf{h}_i and $i = 1 \cdots L$ transmit antennas for MRC and MMSE can be expressed as

$$SINR_i^{MRC}(p_1 \cdots p_L) = p_i \mathbf{h}_i^H \mathbf{h}_i \cdot \sigma^{-2} \quad (4)$$

$$SINR_i^{MMSE}(p_1 \cdots p_L) = p_i \mathbf{h}_i^H [\sigma^2 \mathbf{I} + \sum_{\substack{l=1 \\ l \neq i}}^L p_l \mathbf{h}_l \mathbf{h}_l^H]^{-1} \mathbf{h}_i \quad (5)$$

The SINR values are frequency-selective and calculated on average for each resource block (RB) which contains a group of adjacent subcarriers in frequency direction and a number of consecutive OFDM symbols in time direction. Note that the calculation of **Eq. (3)** and **Eq. (5)** for a system with 2 transmit and 2 receive antennas involve the inversion of a 2×2 matrix for each subcarrier. This is a technical challenge in real-time systems. The update rate for channel equalization, **Eq. (3)**, in our implementation is 0.5 ms.

B. Multi-User MIMO MAC

Frequency dependent multi-user scheduling is implemented on a longer time-scale at the MAC. In our implementation **Eq. (4)** and **Eq. (5)** are updated every 10 ms, within a so-called radio frame (RF). Frequency dependent scheduling allows us to exploit the resources in a broadband OFDMA system in an optimized way, by allocating resource blocks (RB) to users with better spectral efficiency. The scheduling algorithm assigns resources in time, frequency and space domains according to a scheduling policy. The result is a resource grant map for each radio frame. The grant map contains information about the targeted user, the modulation and coding scheme (MCS), and the spatial mode used on each RB. The principal system implementation is shown in **Fig. 1**.

An essential requirement for adaptive resource scheduling is the existence of reliable feedback channels. Feedback channels are implemented using rate 1/2 channel coding. Diversity is maximized by transmission over distributed resources in the frequency domain. The uplink receiver is always in MRC

mode for feedback channels to ensure a more reliable transmission. The SINR values are calculated according to **Eq. (4)** and **Eq. (5)** in real-time, quantized and transmitted over the feedback channel in the uplink to the base station (BS). The SINR feedback is decoded at the BS and used as input for the scheduling algorithm. Note that approximately 1 % of the total uplink RBs are actually used to provide the feedback for one terminal in our experiments.

The implemented scheduling policy is a proportional fair scheduler according to [3], which additionally incorporates a fairness utility function for the scheduler input. The scheduler keeps track on the average rate \mathbf{R}_k^j of each user k on resource j over a fixed window $t_c = 128 * 10 \text{ ms}$, where 10 ms is the duration of a radio frame (RF). \mathbf{Q}_k^j is the supportable sumrate of user k on a specific resource block j . The proportional fair scheduler assigns in time slot t_c the resource to the user \tilde{k} with the largest fraction:

$$\frac{\mathbf{Q}_{\tilde{k}}^j(t)}{\mathbf{R}_{\tilde{k}}^j(t)} \quad (6)$$

The supportable sumrate is $\mathbf{Q}_k^j = \mathbf{Q}_{tx_1}^j + \mathbf{Q}_{tx_2}^j$, where $\mathbf{Q}_{tx_i}^j$ is the resource j on transmit antenna i . In (6), \mathbf{Q}_k^j is updated for every resource block (RB). The number of available resource blocks (RB) per antenna is 48. The long-term rate \mathbf{R}_k^j for timestamp t is calculated by

$$\mathbf{R}_k^j(t) = \sum_{T=t-t_c}^t \mathbf{Q}_k^j(T) \quad (7)$$

III. REAL-TIME IMPLEMENTATION

PHY and MAC for BS and UE have been implemented on a standard signal processing platform previously used for 1 Gbit/s MIMO-OFDM transmission experiments [1]. The new MAC layer connects via 1 Gbit/s Ethernet to the IP layer.

The implemented physical layer (PHY) is similar to the currently discussed 3G-Long-Term-Evolution (LTE). Differences concern only synchronization, pilot signals and the size of resource blocks (RB). The implementation follows working assumptions in the LTE study item in November 2005 [4]. For the downlink, 2 transmit antennas at the base station (BS) and 2 receive antennas at the user equipment (UE) are used. The FFT/IFFT size is 2048 points. One transmission time interval (TTI) spans 0.5 ms or 7 OFDM symbols with 1200 subcarriers each. The cyclic prefix/guard interval is 4.7 μs . 20 consecutive TTIs form a radio frame with a length of 10 ms. In the uplink, DFT pre-coding is used with a number of fixed sizes $n=25, 50, 75, 100, 200, 300, 400, 600, 1200$. Note that these numbers are integer fractions of 1200.

Uplink (UL) and downlink (DL) signals are transmitted simultaneously in FDD mode in the UMTS extension band at 2.68 GHz for DL with a bandwidth of 20 MHz. The UL uses 2.53 GHz carrier frequency with a reduced bandwidth of 5 MHz to improve the reliability of feedback signals. RF front-ends include duplex filters, mixers, local oscillators and automatic gain control. IQ imbalance correction and analogue

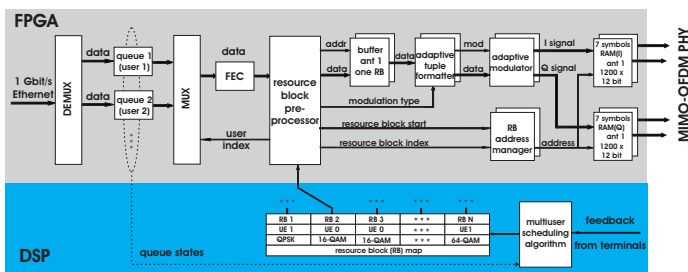


Fig. 2. Real-Time Multi-User MAC

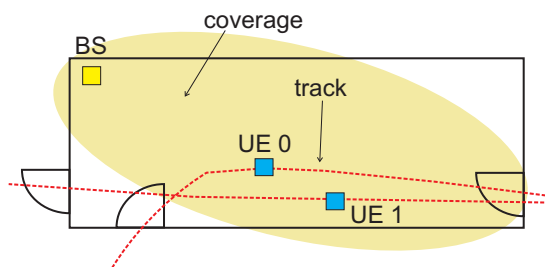


Fig. 3. Indoor Scenario

filtering are so precise that MIMO-OFDMA transmission with up to 64-QAM modulation is possible in both directions. Frontend and base band processing are digitally coupled via parallel link at the UE side and via serial link at the BS. The serial link protocol used at the BS is CPRI 1.2 Gbit/s. The PHY chain includes coarse and fine synchronization, channel estimation, MIMO equalization as well as a simplified FEC based on convolutional coding.

The resource map is transmitted as broadcast over the control channel in the downlink. It is decoded by each UE. The receiver picks out signals on granted resources and feeds them into the FEC.

A. Multi-User MIMO MAC

The scheduling decision must take into account the size of physical data blocks and the applied code rate. We have used data blocks of 432 bits at the input of the forward error correction (FEC). Resource blocks (RB) at the PHY cover 25 subcarriers and 1 TTI (7 OFDM symbols). The number of resource blocks granted for a given data block may vary according to the variable modulation and coding scheme and scheduling policy.

Fig. 2 illustrates the real-time multi-user MIMO MAC processor. The flexible resource mapping in the user plane is fully pipelined and implemented in a FPGA. The flexible scheduling algorithm is part of the control plane and implemented on a DSP. The interface between both components is established by a common memory block which contains the resource map.

IV. MEASUREMENT SCENARIOS

We have deployed a multi-user MIMO scenario with one base station (BS) and two user equipments (UE). There was no interference from other BSs. Measurements were conducted in indoor office and outdoor scenarios.

A. Indoor Scenario

The indoor scenario consisted of a typical rectangular office room of size 20 m x 8 m x 3 m, shown in Fig. 3. The room contained typical office furniture, e.g. chairs, tables and computers. The room had three doors at each side and a window front on the 4th side. The BS was located in the corner of the room. Both UEs were moved along predefined routes through the room using a constant velocity of approximately 1 m/s. All antennas are cross-polarized.

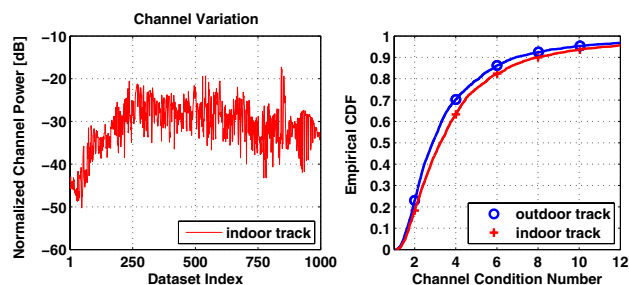


Fig. 4. Indoor and Outdoor Channel Characteristics

B. Outdoor Scenario

The outdoor scenario was a typical suburban scenario. The scenario is characterized by NLOS and multipath propagation with houses of 6-9 m height in the surrounding area. The BS antenna covered a single 120 ° sector and was mounted at a window of a modern office building. For the BS antenna, a commercial cross-polarized outdoor antenna (+/-45°) with 11 dBi gain and built-in down-tilt of 3° was used. The antenna height was 15 m above the ground and above rooftop of the surrounding buildings.

The UE antennas were installed at 2 m height on a mobile trolley. A fixed route was taken on several runs with constant speeds of 1 m/s. The path loss on the measurement track ranged from -80 db to -60 db. The distance between BS antenna and UE was between 30 and 80 m.

V. RESULTS

A. Channel Characteristics

The measured pathloss over time for the indoor scenario is shown in Fig. 4 (left). The channel was measured at each user equipment (UE). The channel condition number is shown in Fig. 4 (right). A small condition number indicates that the channel is more suitable for MIMO transmission. It can be observed, that the outdoor channel is better conditioned. The reason for this is that the outdoor scenario is NLOS, while we have free LOS to the BS in the indoor scenario.

B. Indoor Results

1) Bit Error Rate: Fig. 5 shows the bit error rate (BER) of UE 0 and UE 1 over time. The target BER of the scheduling algorithm was set to $2 \cdot 10^{-2}$. It can be observed that this requirement is almost always fulfilled with some fluctuation

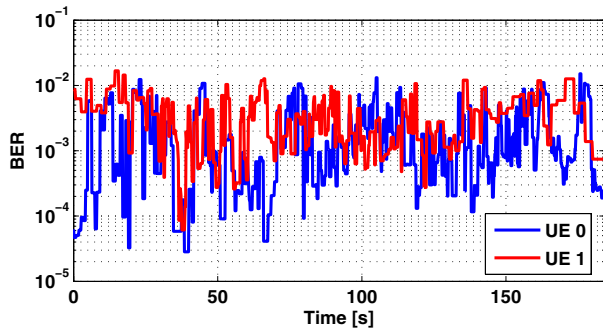


Fig. 5. Indoor: BER over Time

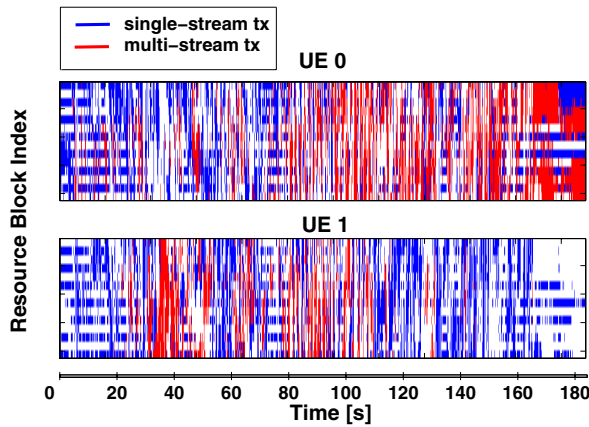


Fig. 6. Indoor: Spatial Mode Selection

towards lower BERs. The fluctuations are caused by the discrete modulation and coding scheme (MCS). If the BER requirement cannot be reached, the next MCS is applied having a reduced data load and hence less errors.

2) *Spatial Mode Selection*: **Fig. 6** shows the resource block (RB) allocation for both UEs over time. The resource block index contains 48 RBs in frequency domain per antenna. The color of each RB indicates the spatial mode assigned by the scheduler to the UE. Blue indicates single-stream, while red indicates dual-stream mode. White indicates no resources assigned to this UE. The allocation table shows that both modes are utilized for both UEs. If two users have the same priority at the same resource, the scheduler assigns the odd resource to UE 0 and the even resource to UE 1. This explains the stripe structure in the allocation plot.

98 % of all RBs are assigned in this scenario, 60 % for single-stream and 38 % for dual-stream transmission. After 160 s, UE 1 was moving out of the BS coverage. Therefore it only supports the lowest MCS level on a few RBs in single-stream mode. Here, the supportable rates on all other RBs were scheduled to UE 0.

3) *Single-Stream Mode*: In the indoor scenario, we have studied the effective SINR seen at the QAM demodulator in more detail. All channel estimates are available at each UE from the broadcasted pilots in the downlink. In order to

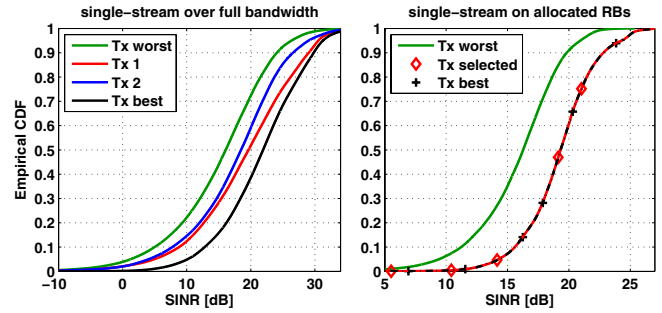


Fig. 7. Single-Stream Scheduler Input (left) and Output (right)

separate the overall path-loss variances during the experiments from the spatial structure of the channel, we have normalized all measured channels before calculating the effective SINR.

Fig. 7 (left) shows the CDF of the SINR according to **Eq. (4)**, considering a fixed single-stream transmission mode over the full bandwidth. The blue and red curves represent the distribution over all timeslots and RBs of the MRC for transmit antenna 1 and 2 in single-stream mode, respectively. The green and black curves show a frequency-selective ordering between the two single-stream options on each RB. We observe that choosing the better antenna in single-stream mode achieves a significant gain for the effective SINR, as compared to a fixed choice of the transmit antenna.

In **Fig. 7 (right)**, we have calculated the same values as in **Fig. 7 (left)**, but only on those resource blocks (RB) actually allocated to the single-stream mode, in competition with multi-stream transmission. The green curve represent the case where the scheduler decides for the worst stream, the black curve where it decides for the best stream. The red curve represents the effective SINR for single-stream transmission selected by the scheduler in our implementation. We observe that the red curve coincides with the black curve meaning that the scheduler always selects the correct single-stream. Note, that in the scheduling algorithm additional constraints like matching the packet data unit (PDU) size with the given resources and the MCS levels have been considered. Obviously, the additional constraints have a negligible effect on the overall system performance.

4) *Multi-Stream Mode*: **Fig. 8** shows similar results for the dual-stream case. The left group of curves represents a dual-stream mode operation and the achieved SINRs assuming the implemented linear MMSE algorithm, according to **Eq. (5)**. Red and blue curves again represent the stream from transmit antenna 1 and 2 which are transmitting data on the same time and frequency resource. In full-bandwidth mode, distributions have a long tail towards low SINR since a second stream has to be separated by the spatial equalizer, which is difficult on some resource blocks (RB). When ordering the two parallel streams according to their SINR on the particular RB, we observe a significant difference between the green and black curves, meaning that in practice the two streams will use a different MCS level for optimal loading.

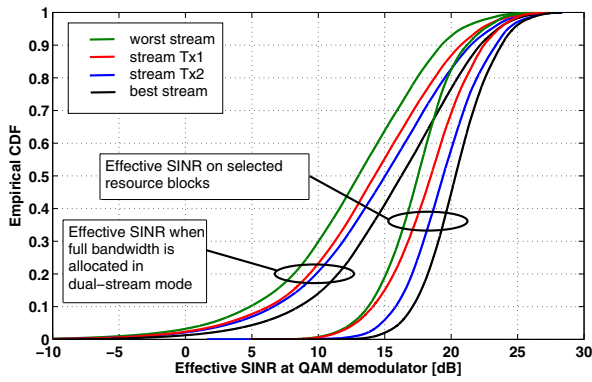


Fig. 8. Multi-Stream Scheduler Input and Output

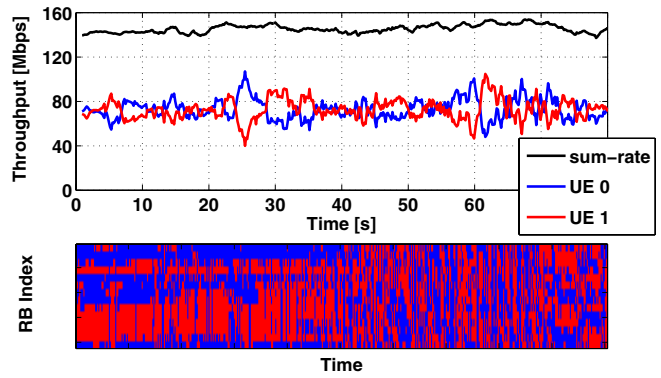


Fig. 10. Outdoor: Throughput over Time (top) and RB-Allocation (bottom)

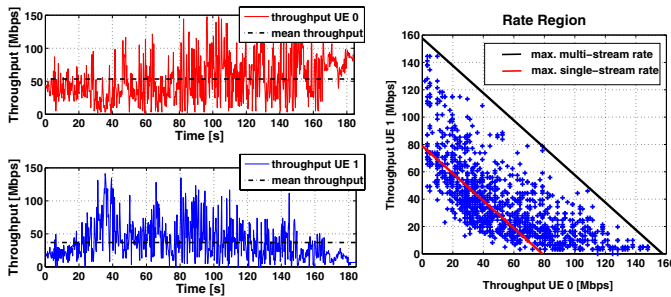


Fig. 9. Indoor: Single-User Throughput and Rate Region

The right group of curves in **Fig. 8** again represent the SINRs achieved in multi-stream mode but only on RBs which were actually selected for multi-stream transmission by the scheduling algorithm, in competition with the single-stream mode. We observe that only channels with a sufficiently high effective SINR ≥ 10 dB are assigned in multi-stream mode. The rightmost black curve represents the better of the two streams.

5) *Throughput*: Throughput results are shown in **Fig. 9**. The left figure shows the single-user throughput over time for both UEs. The average rates are 54 Mbps for UE 0 (top) and 38 Mbps for UE 1 (bottom) in the indoor scenario. The right figure shows the rate region. Each point represents the rate of UE 0 and UE 1 for one radio frame. The red line in the rate region plots defines the maximum single-stream rate, the black line the maximum multi-stream rate. From the rate region plot, we can evaluate the fairness achieved with the proportional fair scheduler. Since the scheduler assigns resources to one UE if the other UE suffers from a bad channel, sometimes all the resources are given to one UE. In most cases, of course, both users are served simultaneously.

C. Outdoor Results - Throughput

The throughput increases in the outdoor measurement due to a higher transmit power and a better channel condition, as shown in **Fig. 10**. In the first part of the measurement, both UEs were not moving. Regarding the resource block

(RB) allocation of each UE during the first 40 s of the measurements, both UEs get an almost static RB assignment: the users are assigned consecutive RBs. Since both UEs were not moving, the channel of each UE remains static and each UE always gets the same RBs in the scheduling list. After about 40 s, both UEs start to move and the channel changes for each UE resulting in a scattered allocation of RBs. The throughput curve shows that the proportional fair scheduler indeed divides resources fair among both users over time and frequency. Each user has a mean throughput of 73 Mbps, which results in a total system throughput of 146 Mbps.

D. Multi-User MIMO

1) *Measurements*: In **Fig. 8** we already observed that if a UE is granted only the better of the two streams while the second stream is allocated to another UE in the cell, a further increase of SINR and therefore also in throughput per allocated stream is possible. Assuming a significant number of other UEs in an SINR range which allows for multi-stream operation, the probability to find another UE which reports its best of the two streams on the other transmit antenna is quite high. If the BS scheduler then allocates the two streams to two different users at the same time, this is a straight forward realization of multi-user spatial multiplexing as it is referred to in 3GPP-LTE in the multi-user downlink. Recent system-level simulations indicate that this multi-user spatial multiplexing mode is one of the drivers for the capacity in the multi-cell scenario with 20 users served in each sector [5].

2) *Simulation*: We have evaluated the achievable gains with multi-user MIMO based on measurements in the indoor scenario in a two user simulation. In order to evaluate the potential diversity gain of multi-user MIMO, we have used the resource requests from both UEs from the indoor measurement, updated the scheduling algorithm and created new resource maps in which two users can be supported in dual-stream mode on the same RB and each user is assigned one of the two streams. Resource requests and scheduling decisions based on the measured feedback are shown in **Fig. 11**. The plots **A-G** show the allocation of resource blocks (RB) over time for two

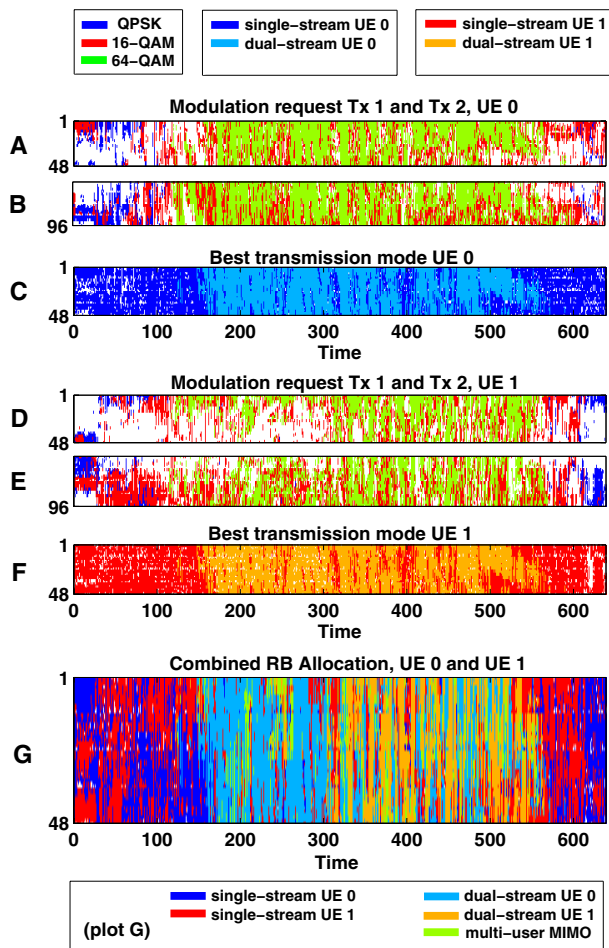


Fig. 11. Scheduler Allocation Input and Output

antennas. Plots **A**, **B**, **D** and **E** show the modulation requests of UE 0 and UE 1 for each transmit antenna at the BS. Blue stands for QPSK, red for 16-QAM and green for 64-QAM RB requests. White represents no modulation request on a particular RB. Plots **C** and **F** show the scheduler decision for the resource allocation in a single-user MIMO scenario. The plots indicate whether the RBs are scheduled using single-stream transmission, which is marked dark blue and red, or multi-stream transmission (MIMO), marked with light blue and orange.

Plot **G** of **Fig. 11** shows the output of the proportional fair scheduler at the BS for the 2 UEs including multi-user MIMO. The RBs marked blue and red are single-stream transmission for UE 0 or UE 1, light blue and orange mark the MIMO decision for the particular user. Notice the overlap region in the central part of plots **C** and **F** where the MIMO mode would be selected frequently for UE 0 and UE 1. The positions in plot **G** with light green color correspond to this particular spatial multiplexing mode where each user is supported on its best stream only. Obviously, multi-user MIMO is sometimes favorable already with two users. Finally, **Table I** summarizes the results from **Fig. 11**. With multi-user MIMO we have a

TABLE I
SPATIAL MODES

Mode	Single-User	Multi-User(2 UEs)
no allocation	13 %	1 %
single-stream	44 %	46 %
dual-stream	43 %	53 % (7 % multi-user MIMO)

10 % gain in dual-stream transmission which mainly results from the fact that the two UEs can be supported on their best stream in multi-user MIMO. With increasing number of users, the scheduler decides more frequently for spatial multiplexing instead of single-stream transmission, which increases the spectral efficiency.

VI. CONCLUSION

In this paper, we have presented a first real-time PHY and MAC implementation for frequency-selective multi-user MIMO using parameters close to the forthcoming 3G LTE standard. It is shown that the very complex MAC functions can be implemented on standard digital signal processing hardware. With a suitable partitioning of the elementary functions, i.e. user plane in hardware and control plane in software, high aggregate data rates of more than 100 Mbit/s can be realized with incredible flexibility for the resource allocation. We have tested the new MAC functions in first indoor and outdoor measurements with two users moving at pedestrian speeds. The results confirm the high potential throughput in real propagation environments due to the combination of frequency-selective resource assignment to multiple users, spatial mode selection and adaptive modulation. Altogether, frequency-selective multiuser MIMO is technically feasible for application in next-generation cellular radio and it implies a significant improvement of the overall system performance.

ACKNOWLEDGMENT

The authors are grateful for sponsoring by the German Ministry of Education and Research (BMBF) and Nokia Siemens Networks in the collaborative research project ScaleNet.

REFERENCES

- [1] V. Jungnickel, A. Forck, T. Haustein, S. Schiffermuller, C. von Helmolt, F. Luhn, M. Pollock, C. Juchems, M. Lampe, W. Zirwas, J. Eichinger, and E. Schulz, "1 Gbit/s MIMO-OFDM Transmission Experiments," in *Proc. of 62nd IEEE Semiannual Vehicular Techn. Conf. (VTC 2005)*, vol. 2, Dallas, USA, September 2005, pp. 861–866.
- [2] T. Haustein, C. Zhou, A. Forck, H. Gabler, C. Helmolt, V. Jungnickel, and U. Kruger, "Implementation of Channel Aware Scheduling and Bit-loading for the Multiuser SIMO MAC in a Real-time MIMO demonstration Test-bed at high Data Rate," in *Proc. of Vehicular Technology Conference. (VTC2004-Fall)*, vol. 2, 2004, pp. 1043–1047.
- [3] P. Viswanath, D. Tse, and R. Laroia, "Opportunistic Beamforming using Dumb Antennas," *IEEE Transactions on Information Theory*, vol. 48, no. 6, pp. 1277–1294, 2002.
- [4] IEEE 3GPP TS 36.211, 36.213, 36.214, V8.0.0, *Physical Channels and Modulation (Release 8)*. [Online]. Available: <http://www.3gpp.org/ftp/Specs/>
- [5] L. Thiele, M. Schellmann, W. Zirwas, and V. Jungnickel, "Capacity Scaling of Multiuser MIMO with Limited Feedback in a Multicell Environment," in *Proc. of 41st Asilomar Conference on Signals, Systems and Computers*. Monterey, USA: IEEE, Nov 2007, invited.